Metrologia

PAPER

Measurements of absolute, SI-traceable lunar irradiance with the airborne lunar spectral irradiance (air-LUSI) instrument

To cite this article: J T Woodward *et al* 2022 *Metrologia* **59** 034001

View the article online for updates and enhancements.

You may also like

- The realization of the NIST detector-based spectral irradiance scale
H W Yoon, C E Gibson and P Y Barnes

- A model for the estimation of global spectral solar irradiance under all-sky conditions for Nakhon Pathom station, Thailand
S Khakhu, I Masiri, R Wattan et al.

- Final report on bilateral comparison APMP.PR-K1.a.1-2008 between KRISS (Korea) and VNIIOFI (Russia): Spectral irradiance from 250 nm to 2500 nm
Dong-Joo Shin, Chul-Woung Park, Svetlana S Kolesnikova et al.

This content was downloaded from IP address 130.113.111.210 on 27/02/2025 at 14:39

IOP Publishing | Bureau International des Poids et Mesures Metrologia
Metrologia **59** (2022) 034001 (9pp) https://doi.org/10.1088/1681-7575/ac64dc

Measurements of absolute, SI-traceable lunar irradiance with the airborne lunar spectral irradiance (air-LUSI) instrument

J T Woodward[1,*], K R Turpie[2], T C Stone[3], S A Gadsden[4], A Newton[4], S E Maxwell[1], S E Grantham[1], T C Larason[1] and S W Brown[1]

[1] National Institute of Standards and Technology, Physical Measurement Laboratory, Sensor Science Division, Gaithersburg, MD 20899, United States of America
[2] Joint Center for Earth Systems Technology, University of Maryland Baltimore County, Baltimore, MD 21250, United States of America
[3] United States Geological Survey, Flagstaff, AZ 86001, United States of America
[4] McMaster University, Hamilton, Ontario, L8S 4L8, Canada

E-mail: john.woodward@nist.gov

Received 2 August 2021, revised 29 March 2022
Accepted for publication 6 April 2022
Published 5 May 2022

Abstract
The airborne lunar spectral irradiance (air-LUSI) instrument is designed to make low uncertainty measurements of the lunar spectral irradiance from an ER-2 aircraft from altitudes above 95% of the atmosphere. Measurements cover the visible and near infrared spectral region (350 nm to 1050 nm) and are traceable to the international system of units. Five demonstration flights were conducted in November 2019 at NASA's Armstrong Flight Research Center. During that campaign, air-LUSI measured the spectral irradiance at lunar phase angles ranging from 10° to 60°. This work provides an overview of the air-LUSI instrument, the lunar irradiance measurements made during demonstration flights, a description of our calibration approach, and summary of the uncertainty budget. Based on the flight results and laboratory measurements, we estimate the instrument is capable of measuring lunar irradiance, propagated to the top-of-the atmosphere, with combined standard uncertainty of 1% ($k = 1$) or less over the spectral region from 450 nm to 980 nm. An examination of the uncertainty budget leads to a path forward toward potentially achieving uncertainties of 0.6% in lunar irradiance over much of the spectral range for future flights.

Keywords: lunar irradiance, satellite calibration, airborne instrumentation

(Some figures may appear in colour only in the online journal)

1. Introduction

Reliable characterization and calibration of on-orbit sensors are two of several key actions necessary to achieve the science objectives identified for current and future space-based sensors that observe the Earth. Historically, sensors have used celestial sources such as the Sun, the stars, and the Moon, as well as sites on the Earth, for trending sensor responsivity changes on-orbit. Each target has limitations and no single approach fully addresses a sensor's *in situ* vicarious calibration requirements. The Moon is an attractive calibration target because the reflectance of the lunar surface is photometrically stable [1], flux levels approximate those from the Earth, and no atmospheric corrections need to be applied to the measurements [2]. While many sources of uncertainty that arise when vicariously calibrating sensors using Earth targets are eliminated, lunar measurements are complicated because the lunar irradiance is a function of the relative positions of the Sun, Moon, and observer (spacecraft) [3]. Consequently, use of the Moon as a calibration target requires a modeled lunar irradiance or reflectance.

[*] Author to whom any correspondence should be addressed.

 © 2022 BIPM & IOP Publishing Ltd Printed in the UK

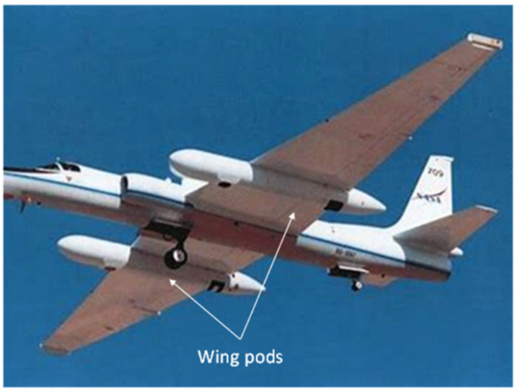

Figure 1. Location of the wing pods on the ER-2 aircraft. The downward facing viewports are rotated 180° for lunar measurements (NASA photo).

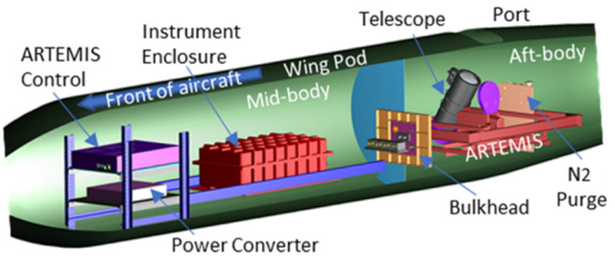

Figure 2. Schematic illustration of air-LUSI mounted in the aircraft wingpod.

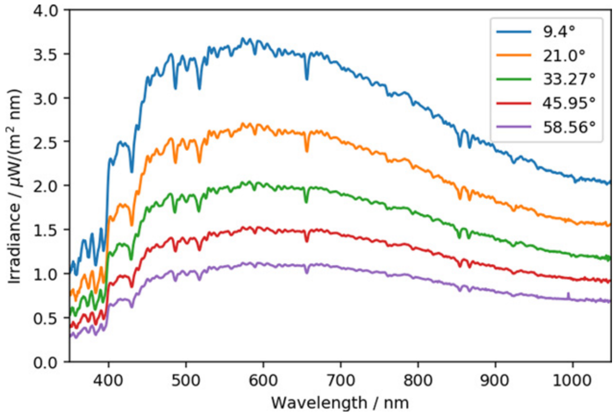

Figure 3. Preliminary mean at-sensor lunar irradiances measured by air-LUSI during demonstration flights in November 2019.

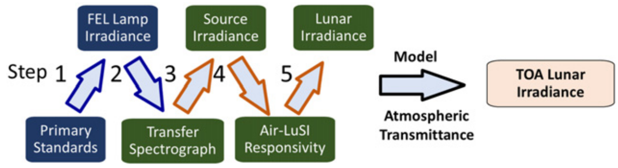

Figure 4. Lunar irradiance measurement chain.

The United States Geological Survey (USGS) has developed the robotic lunar observatory (ROLO) model of the top-of-the atmosphere (TOA) lunar reflectance, which accounts for changes in lunar irradiance as a function of the relative positions of the Sun, Moon, and observer (spacecraft). The USGS ROLO model [3] and the global space-based inter-calibration system implementation of the ROLO model (the GIRO model [4]) are the current most precise knowledge of lunar spectral reflectance. However, the current absolute uncertainties in the ROLO model cannot be demonstrated to better than approximately 5%, with a 3% to 4% uncertainty component coming from the atmospheric transmittance used in the stellar-based calibration of the ROLO telescope. Finally, measurements used to develop the ROLO model were not traceable to the international system of units (SI) and hence the model itself is not SI-traceable. While the Moon is used frequently as a relative calibration source by space-borne sensors to monitor temporal changes in instrument responsivity, it is not used currently as an absolute calibration source.

Geometries encountered for satellite sensor measurements of lunar irradiance are quite different from those seen in measurements of the Earth's reflectance. Satellite sensors in low earth orbit (LEO) measure the reflected radiance from the Earth from altitudes of less than 2000 km. Typically, the Earth completely fills the sensor's field of regard. In contrast, the Moon is several hundred times more distant, the Moon subtends an angle of 0.5° and underfills the sensor field of regard. Sensors typically acquire lunar radiance measurements that then need to be processed into irradiance measurements. For low uncertainty measurements, potential sources of errors in lunar measurements by satellite sensors should be identified and their impact on measurements quantified. For example, to convert from a radiance image of the Moon to a lunar irradiance measurement requires knowledge of each sensor element's solid angle, as well as the oversampling factor for oversampled lunar images such as those acquired by line-scanning sensors. Finally, a spacecraft maneuver is typically required for LEO sensors to view the Moon and there may be a correction for a sensor's change in altitude compared to its Earth viewing position.

Airborne lunar spectral irradiance (air-LUSI) measurements, corrected for residual atmospheric attenuation, are designed to provide a data set of low uncertainty, SI-traceable, TOA lunar irradiances at known lunar phase and libration angles to be compared and integrated with other lunar irradiance data sets. The air-LUSI program seeks to improve the Moon's utility as an absolute calibration target by reducing the uncertainty in the modeled spectral irradiance and tying measurements to the SI. Among other applications, these measurements may be used to assess potential biases in lunar models and lunar observations by satellite sensors.

The goal of the Demonstration Flight Campaign was to validate the performance of the instrument. As part of the analysis, a relevant uncertainty budget and a path forward toward expected uncertainties during operational flights was developed. Results from lunar measurements taken during flights on five successive nights in November 2019, corresponding to median phase angles of 9.4°, 21.0°, 33.27°, 45.95°, and 58.56°, are presented; an uncertainty budget is developed showing a measurement uncertainty less than 1% over much of the spectral range; and a path forward toward potentially achieving an uncertainty of 0.6% over much of the spectral range is given.

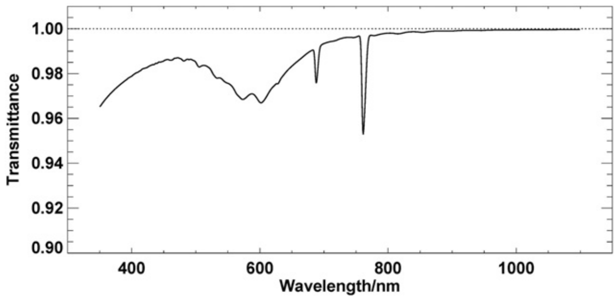

Figure 5. Nominal atmospheric transmittance for air-LUSI demonstration flight 4, Nov. 14, 2019. Data were derived from a MODTRAN spectrum convolved with the air-LUSI spectrograph line shapes, with MODTRAN configured for a slant path to space from the air-LUSI flight altitude and lunar zenith angle.

2. Air-LUSI instrument

Air-LUSI is designed to fit in one of two instrument pods located under the wings of an ER-2 aircraft, illustrated in figure 1. Each pod has three sections: a fore-body, a mid-body and an aft-body; air-LUSI is installed in the mid-body and the aft-body. During flight, the mid-body is kept at a minimum pressure of 33.7 kPa (1/3 atm) and temperature of at least 0 °C. The aft-body is open to the environment and during lunar measurements is at an atmospheric pressure of approximately 6.1 kPa (0.06 atm) and can reach temperatures as low as −70 °C. The downward facing port seen in figure 1 is rotated to be upward facing for lunar observations and has no window.

The air-LUSI instrument is divided into three subsystems, the irradiance instrument subsystem (IRIS) [5] to measure the lunar irradiance, an autonomous, robotic telescope mount instrument subsystem (ARTEMIS) [6] to maintain the telescope alignment with the Moon; and a high-altitude ER-2 adaptation subsystem (HERA) to protect components from the extreme cold and low pressure environment encountered during flight and from moisture condensation during descent. A schematic diagram of air-LUSI mounted in the aircraft is shown in figure 2.

2.1. The IRIS sub-system

The IRIS sub-system consists of a non-imaging telescope [7] located in the aft body of the wing pod mounted on the ARTEMIS tracking system. Incident flux is collected by the telescope's integrating sphere receiver (ISR) and fiber-coupled to a spectrograph housed in an instrument enclosure located in the mid-body of the wing pod. A second optical fiber is used to couple light from an LED validation source located in the instrument enclosure to the ISR. Finally, there is an unfiltered Si photodiode located on the ISR wall to provide a measure of the total integrated flux in the ISR. The spectrograph covers the spectral region from 300 nm to 1100 nm with a 3.7 nm bandpass and a 0.8 nm pixel-to-pixel spacing. To improve the signal-to-noise ratio, the detector array at the focal plane of the spectrograph is cooled to a temperature of −10 °C. The LED validation source uses a green LED peaked at 560 nm with a useable signal to noise level from 480 nm to 700 nm. A fused 90%/10%, 1 × 2 fiber-optic splitter sends 90% of the flux from the LED to the ISR on the IRIS telescope and 10% to a photodiode inside the instrument enclosure that monitors the integrated output of the LED source. Measurements by the spectrograph of the LED flux introduced into the ISR are made during the ascent and descent of each flight and used to assess possible instrument responsivity changes between ground calibration and lunar measurement. The LED source is shuttered during the lunar measurements.

In addition, the instrument enclosure houses transimpedance amplifiers for the two photodiodes, the control computer, relay switches for pilot communication, and a data logger. The front face of the enclosure accommodates four feedthroughs for signals, power, and communication.

2.2. The Artemis sub-system

The ARTEMIS sub-system was designed to control the pointing of the IRIS telescope to observe the Moon through a windowless aperture in the aft-body of the wing pod. It can track the Moon over lunar elevations between 40° and 77°. A camera mounted on the telescope is used to track the Moon at a tuned location in the x–y camera coordinates based on telescope line-of-sight calibrations. Tracking error shifts in the lunar image of a single pixel corresponds to an angular offset of 0.053°. To avoid vignetting of the incident lunar irradiance, the tracking error was required to be less than 0.5° [7]. Linear actuators control the positioning of the telescope in orthogonal axes. A machine vision-based proportional–integral–derivative controller was designed to enable tracking of the Moon with a goal of reaching sub-pixel errors for both axes [8].

2.3. The HERA sub-system

The HERA sub-system provides thermal management to protect components from the extreme cold and low pressures encountered during flight. Heaters were located on the telescope ISR; the actuators that controlled telescope pointing; and the cables, electrical and optical, that run from the mid-body of the wing pod to the telescope located in the aft-body. Thermocouples measure the temperature in the instrument enclosure, the aft-body pod, the shell enclosing the ISR, and inside the aft-body fiber bundle. Heaters and control thermostats were also located on the instrument enclosure to maintain the spectrograph and electronics at temperatures warmer than 20 °C.

3. Demonstration flights

The instrument was successfully integrated into a wing pod of an ER-2 research aircraft at NASA's Armstrong Flight Research Center. Five demonstration flights were conducted on successive nights in November 2019 at median lunar phase angles of 9.4°, 21.0°, 33.27°, 45.95°, and 58.56°, respectively. Each flight consisted of a 40 min ascent, 40 min of lunar data collection above 20 km altitude, and a 40 min descent. The mean at-sensor lunar irradiances from each night of measurements are shown in figure 3.

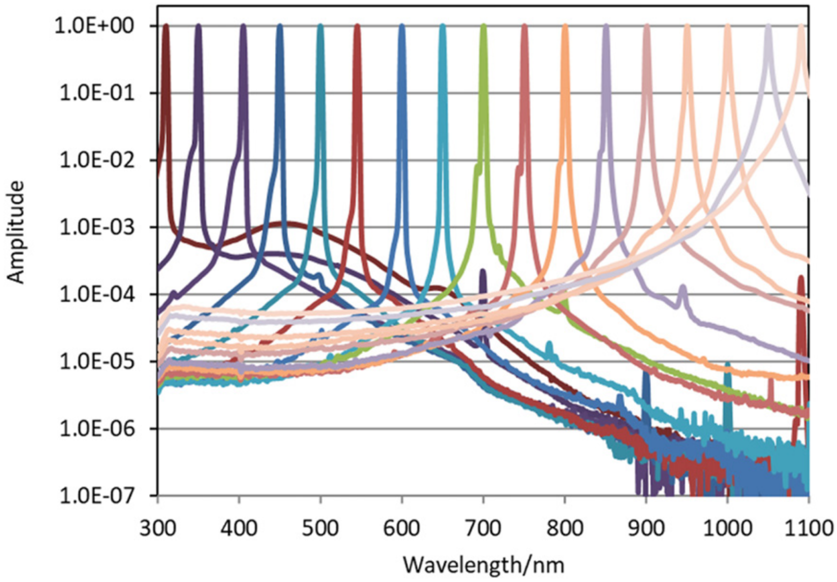

Figure 6. Air-LUSI IS and spectrograph response when illuminated by laser lines of various wavelengths normalized to a peak value of 1. The subset of spectra shown demonstrate the stray light in the spectrograph and the change in bandpass with wavelength.

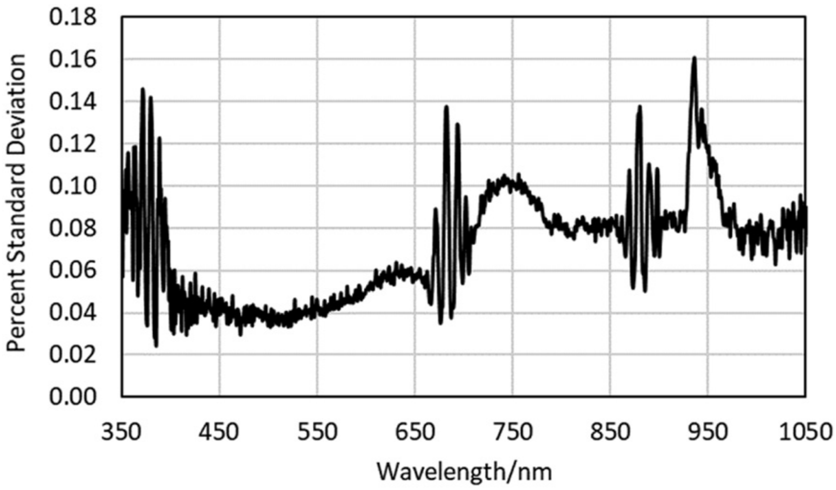

Figure 7. The percent standard deviation in TS irradiance responsivity calibrations to the FEL lamp before and after deployment for the demonstration flights.

The shutter on the LED validation source failed prior to the first flight and the LED was not used on the first four flights. For the fifth flight we modified the control program so that the LED would be on during assent and be powered off during lunar acquisition. Data from a pressure sensor located in the instrument enclosure indicate that it did not hold ground pressure while in flight. Data from the LED validation source and the spectrograph indicate a variation in throughput of the ISR with temperature in excess of our expectations. Each of these anomolies is discussed is section 5.

4. Air-LUSI calibration and uncertainty approach

Development of an uncertainty budget following an analysis of the Demonstration Flight Campaign is useful for directing improvements to the instrument in preparation for future flights. While the analysis of each uncertainty component is beyond the scope of this manuscript, a discussion of principal components is presented.

The measurement chain for an air-LUSI lunar irradiance measurement is shown in figure 4. SI-traceability is maintained through a multistep process where a transfer standard (TS) spectrograph was characterized and calibrated at NIST and used in the field to transfer the SI scale to air-LUSI. FEL-type lamps hold the NIST spectral irradiance scale [9] (step 1). In step 2, the TS spectrograph measured the known FEL irradiance (FEL E) to yield a spectral irradiance responsivity (TS-R). Steps 3 and 4 were performed with the instrument loaded into the ER-2 in the hangar at Armstrong Flight Research Center. The spectral irradiance scale was transferred to the IRIS instrument prior to each flight. In step 3, the irradiance of a lamp-illuminated, 30 cm integrating sphere (IS)

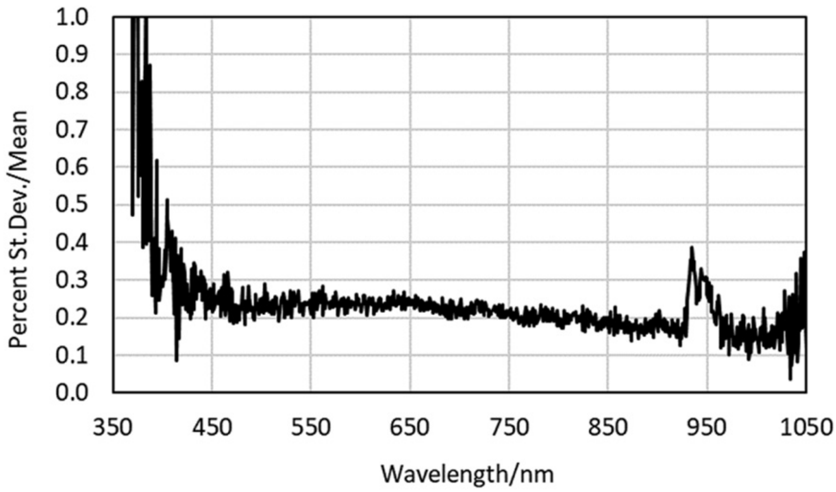

Figure 8. The standard deviation of the mean of the IRIS irradiance responsivity calibrations before each flight and after the final flight.

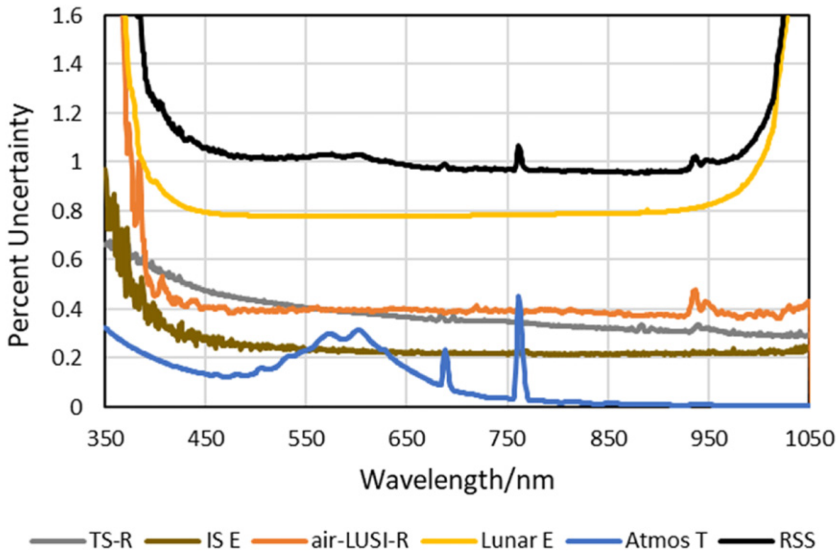

Figure 9. TOA lunar irradiance uncertainty budget by measurement: the transfer standard responsivity (TS-R), the integrating sphere irradiance (IS E), the air-LUSI irradiance responsivity (LUSI-R), lunar irradiance (Lunar E) and the atmospheric transmittance (τ-TOA). RSS refers to the root-sum-square of the individual uncertainty components.

calibration source was measured by the TS to yield the IS irradiance (IS-E). Air-LUSI then measured the IS calibration source in step 4. The distances from the calibration source to the TS and to the air-LUSI telescope were used together with the inverse square law for irradiance to yield the air-LUSI irradiance responsivity (LUSI-R). During step 4, air-LUSI also measured the LED validation source and separately a HgNe lamp. In step 5, IRIS measured the lunar irradiance at defined phase and libration angles from the ER-2 aircraft above 20 km. The ROLO model is used to reference the set of measurements, taken over a 40 min period, to a single time point. Finally, MODTRAN is used with models of atmospheric transmittance to propagate the air-LUSI lunar measurements to the TOA for comparisons with models and sensor measurements of lunar irradiance and reflectance. Figure 5 shows the MODTRAN calculated transmittance, $\tau_{\mathrm{TOA},}$ for flight #4.

Following the measurement chain in figure 4, the measurement equation can be expressed as:

$$E_{\mathrm{Moon}}^{\mathrm{TOA}} = \frac{1}{\tau_{\mathrm{TOA}}} \frac{S_{\mathrm{LUSI}}^{\mathrm{Moon}} T}{S_{\mathrm{LUSI}}^{\mathrm{IS}}} \left(\frac{D_1}{D_2}\right)^2 \frac{S_{\mathrm{TS}}^{\mathrm{IS}}}{S_{\mathrm{TS}}^{\mathrm{FEL}}} E_{\mathrm{FEL}}, \tag{1}$$

where S is the signal measured by the instrument in the subscript while observing the source in the superscript, τ_{TOA} is the atmospheric transmission from air-LUSI to the Moon, D_1 and D_2 are the distances of the TS and air-LUSI from the IS calibration source, T is the ratio between the responsivity of air-LUSI during lunar acquisition and during ground calibration, and E_{FEL} is the irradiance of the FEL lamp used to calibrate the TS. Other than D_1 and D_2, all the components are wavelength dependant. Ignoring potential covariances, the combined standard uncertainty given by equation (2) is the root-sum-square (RSS) of the individual uncertainty budgets

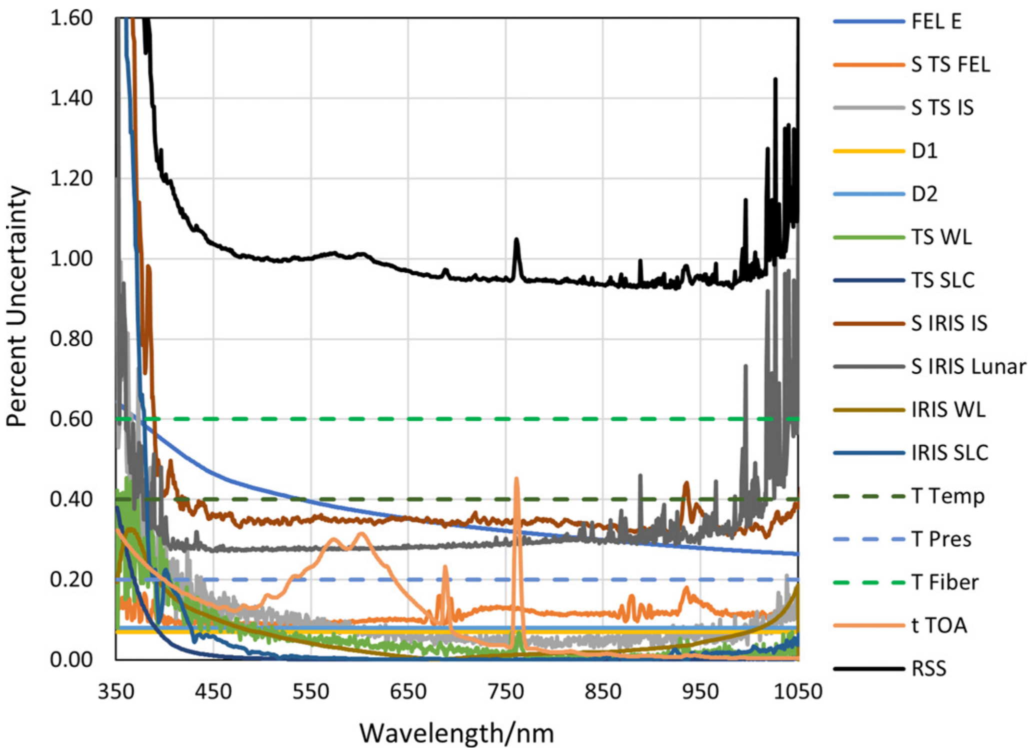

Figure 10. TOA lunar irradiance uncertainty budget by component as a function of wavelength.

Table 1. Uncertainty components for demonstration flights at selected wavelengths.

Component	Uncertainty/%		
	450 nm	650 nm	850 nm
E-FEL	0.46	0.35	0.30
S TS FEL	0.09	0.10	0.12
S TS IS	0.12	0.06	0.04
Distance 1	0.07	0.07	0.07
Distance 2	0.08	0.08	0.08
TS WL	0.11	0.04	0.01
TS SLC	0.01	0.00	0.00
S IRIS IS	0.36	0.35	0.33
S IRIS lunar	0.27	0.28	0.30
IRIS WL	0.10	0.01	0.02
IRIS SLC	0.06	0.00	0.01
T, Temperature	0.40	0.40	0.40
T, Pressure	0.20	0.20	0.20
T, Fiber coupling	0.60	0.60	0.60
τ TOA	0.13	0.15	0.02
RSS	**1.04**	**0.97**	**0.93**

for each component in equation (1):

$$\left(\frac{\mu_c^{\mathrm{TOA}}}{E_{\mathrm{Moon}}^{\mathrm{TOA}}}\right)^2 = \left(\frac{\mu_{\mathrm{E}}}{E_{\mathrm{FEL}}}\right)^2 + \left(\frac{\mu_{\mathrm{Sft}}}{S_{\mathrm{TS}}^{\mathrm{FEL}}}\right)^2 + \left(\frac{\mu_{\mathrm{Sit}}}{S_{\mathrm{TS}}^{\mathrm{IS}}}\right)^2 + \left(\frac{\mu_{\mathrm{Sil}}}{S_{\mathrm{LUSI}}^{\mathrm{IS}}}\right)^2 + \left(\frac{\mu_{\mathrm{Sml}}}{S_{\mathrm{LUSI}}^{\mathrm{Moon}}}\right)^2 + \left(\frac{\mu_{\tau}}{t_{\mathrm{TOA}}}\right)^2 + \left(\frac{\mu_{\mathrm{T}}}{T}\right)^2 + 2\left(\frac{\mu_{D1}}{D_1}\right)^2 + 2\left(\frac{\mu_{D2}}{D_2}\right)^2. \quad (2)$$

Within each uncertainty component, μ_i, are a number of components whose sensitivity components need to be derived along with their magnitudes. Common measurement uncertainty components to be considered include reproducibility, repeatability, measurement, and alignment of an instrument to a source. Each spectrograph made two measurements, the TS measured the FEL and then the IS and air-LUSI measured the IS and then the Moon, and thus there are some covariant terms not shown in equation (2). These include wavelength scale, linearity and stray or scattered light in the spectrograph.

Both the air-LUSI and TS spectrographs were characterized for stray light, signal linearity, and the change in responsivity with temperature. The stray light characterization was performed using a tunable laser to illuminate the spectrographs at 5 nm intervals across the spectral range [10]. A subset of the resulting spectra are shown in figure 6. The spectrograph wavelength scales were derived from measurements of the laser wavelengths used in the stray light characterization and the relative spectral response of the spectrographs and have an uncertainty of 0.05 nm. The measurements of the laser lines also provide bandpass information as a function of wavelength. The signal linearity was measured using a beam conjoiner methodology [11]. Measurements of the calibration IS and HgNe penlamp with the spectrograph at different temperatures provided the temperature sensitivity coefficients for the irradiance responsivity and wavelength scale.

Regarding temporal stability, the spectrographs have demonstrated an 0.02% stability in the laboratory [12]. The TS spectrograph holds the irradiance responsivity scale and its temporal stability over the course of a deployment was assessed by comparing calibrations performed before and after

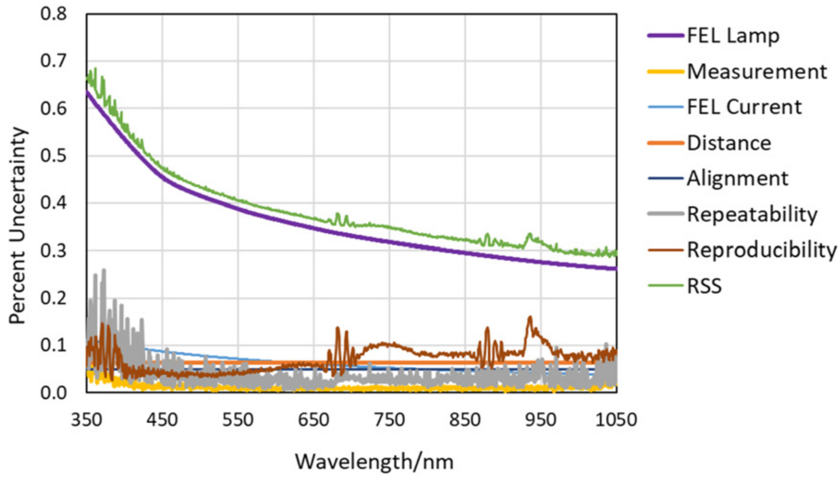

Figure 11. Components in the TS responsivity uncertainty budget and their RSS.

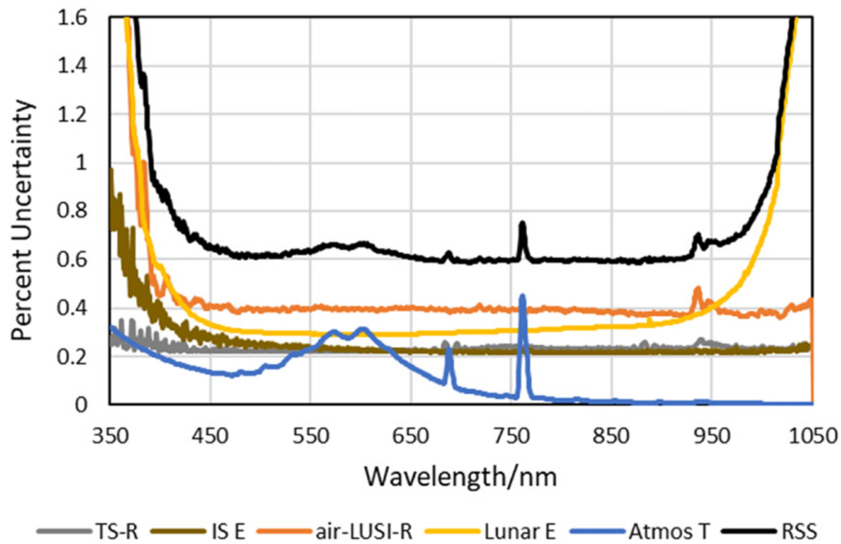

Figure 12. Estimated achievable uncertainty in TOA lunar irradiance by future air-LUSI flights, by measurement: the transfer standard responsivity (TS-R), the integrating sphere irradiance (TS-E), air-LUSI responsivity (air-LUSI-R), and the atmospheric transmittance (τ-TOA).

deployment as seen in figure 7. In figure 8, we show the stability of the IRIS irradiance responsivity by plotting the standard deviation of the mean of calibrations performed before each flight and after the final flight. Its temporal stability between ground calibration and in-flight measurements of the lunar irradiance was only monitored using the LED validation source for the final flight.

To test the radiometric performance of the IRIS system and calibration sphere an inverse square test was performed by measuring the flux from the IS calibration source at a series of distances from 10.5 m to 16.5 m at 1 m intervals. The distance from the telescope aperture to a faceplate on the IS aperture was measured with a laser range finder. The spectrally integrated flux was fit to the inverse square law modified for the finite aperture of the IRIS telescope and the IS. The resulting fit agreed with the thickness of the faceplate to within 2 mm with an uncertainty $\pm$11 mm. Calibrations were performed at a distance between 15 m and 16 m.

5. Results and discussion

While our target uncertainties in the lunar irradiance are 0.5% or lower, an SI-traceable, TOA lunar irradiance data set with uncertainties less than 1% meets many sensor calibration uncertainty requirements and includes the ability to bring inter-consistency between contemporary missions and across series of missions by using a common, stable reference. The air-LUSI measurements may also help resolve questions about the origin of differences between sensor measurements of the lunar irradiances and model predictions.

There are negligible differences in the uncertainty budgets of the five flights. The average root-mean-square Error tracking error across all flights was 0.1°, well below the 0.5° requirement [7, 8]. Estimated uncertainties in the TOA lunar irradiance for flight 5 are given in figure 9. The combined standard uncertainty is less than 1% from 450 nm to 980 nm.

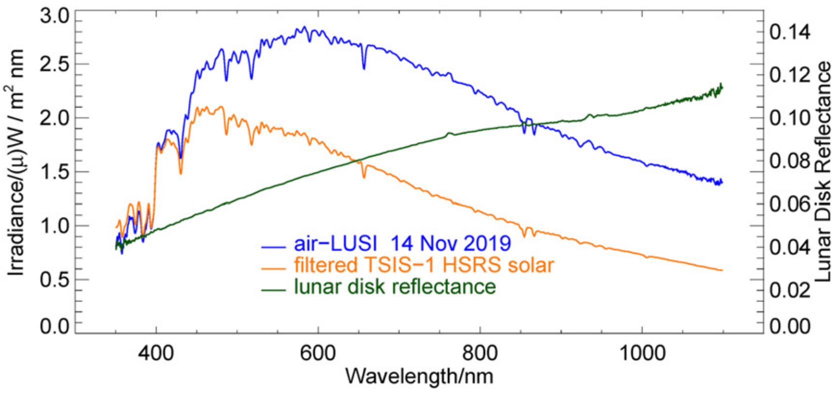

Figure 13. The TOA air-LUSI lunar irradiance measured on the night of Nov. 14, 2019 was converted to a lunar reflectance using the TSIS-1 hybrid solar reflectance spectrum yielding a smooth lunar reflectance curve. The scale on the left axis is μW/m^2 nm for lunar irradiance and W/m^2 nm for solar irradiance.

Figure 10 shows the lunar irradiance uncertainty budget broken out by component and table 1 has numeric values for select wavelengths. The three uncertainty components shown by dashed lines result from unexpected conditions encountered during flight. There was a loss of pressure in the instrument enclosure due to leaks in the electrical feed-throughs, an instability in the fiber coupling, and a temporal instability in the throughput of the telescope RIS attributed to a phase transition in the polytetrafluoroethylene sphere material at 19 °C impacting the transmittance of the IS [13]. This effect, monitored by the LED, is estimated to be 0.4% based on the data from flight 5. There was no spectral dependance over the wavelength range of the LED. After the campaign, we tested the effect of the pressure loss by partially evacuating the environmental enclosure while measuring the calibration IS and assigned an 0.2% uncertainty. No spectral shift was seen in spectra of a HgNe penlamp due to the reduced pressure.

There was a measured change in the instrument irradiance responsivity after it was loaded on the aircraft and under aircraft power. While the reproducibility of instrument calibrations between flights was very good, we do not have a complete understanding of the origin of the instrument responsivity change during loading and unloading the instrument from the aircraft and its potential impact on the in-flight measurements. One possible source of this change is an instability in the optical fiber bundle coupling to the spectrograph that may have allowed it to shift during rough handling. We assign an additional 0.6% type B uncertainty to the transfer ratio between ground and airborne IRIS responsivity, T, for fiber coupling instability. We emphasize that because the instrument is recalibrated before and after every flight and because we can monitor the throughput of the IS during taxiing and flight, a change in calibration outside of the series of flights does not affect our uncertainty budget.

The next largest component in the uncertainty budget is the calibration of the TS. The uncertainty in the distributed irradiance scale of the FEL lamp is the dominant uncertainty component in the calibration of the TS, figure 11. To reduce the uncertainty in the calibration of the TS, we are moving from a lamp-based calibration to a detector-based calibration. The estimated uncertainties in the detector-based calibration are spectrally invariant with an estimated band integrated uncertainty of 0.2% for each element in the detector array [14]. Figure 12 shows the anticipated impact on the uncertainty in the TOA lunar irradiance, implying we may be able to achieve an uncertainty of approximately 0.6% from 450 nm to 950 nm.

In preparation for a March 2022 flight campaign, the instrument is slated to undergo tests in an atmospheric chamber to better understand its performance during demonstration flights. The vacuum leaks in the instrument enclosure have been repaired and a new RIS has been designed with better thermal distribution and control. The current temperature control of the IS is ±5 °C centered at 20 °C. To reduce the uncertainty in the IS temporal stability, the temperature control range of the heaters will be reduced to ±2 °C around a slightly elevated temperature of 25 °C, thereby avoiding the phase transition at 19 °C [13].

Because the lunar reflectance is effectively invariant [1], high-accuracy lunar irradiance measurements are most useful as input for developing models that predict the lunar irradiance under different viewing geometries. As a check on the air-LUSI wavelength scale, the air-LUSI irradiance measurements were converted to reflectance using the TSIS-1 hybrid solar reference spectrum [15] filtered to the spectrograph line shapes. Results are shown in figure 13, where the derived reflectance spectrum exhibits the smooth spectral shape expected for the Moon. Any error in the wavelength scale or mismatch to the solar spectrum would result in sharp features in the reflectance spectrum near regions of sharp features in the solar spectrum; no such features are seen in the reflectance.

In summary, five demonstration flights occurred during the deployment of air-LUSI to NASA's Armstrong Flight Research Center in November 2019 covering approximate phase angles from 10° to 60°. The measurements were tied to the TS spectrograph and are traceable to the SI. An uncertainty budget was developed and, given our current knowledge, the combined standard uncertainties in the TOA lunar irradiance are estimated to be 1% or less over the spectral range from 450 nm to 980 nm. Finally, an examination of the uncertainty budget gives direction to a path to potentially reduce the uncertainties to approximately 0.6% from 450 nm to 950 nm for future flights.

Acknowledgments

The air-LUSI team would like to thank staff at the Hawk Institute for Space Sciences for their thermal management and control design and staff at NASA's Armstrong Flight Research Center for their tremendous support during Flight Operations. We thank our colleagues Carol Johnson, Howard Yoon and Yuqin Zong for their assistance with characterizing the air-LUSI and Transfer spectrographs. Funding was provided by NASA's Earth Science Technology Office and Earth Science Division under Grant NNH16ZDA001N-AITT and the National Institute of Standards and Technology (NIST). Certain commercial equipment, instruments, or materials are identified in this paper in order to specify the experimental procedure adequately. Such identification is not intended to imply recommendation or endorsement by NIST, nor is it intended to imply that the materials or equipment identified are necessarily the best available for the purpose.

ORCID iDs

J T Woodward https://orcid.org/0000-0001-7719-3187
T C Stone https://orcid.org/0000-0001-5088-3495
S A Gadsden https://orcid.org/0000-0003-3749-0878
T C Larason https://orcid.org/0000-0001-5249-6317

References

[1] Kieffer H H 1997 *Icarus* **130** 323–7
[2] Stone T C, Kieffer H, Lukashin C and Turpie K 2020 *Remote Sens.* **12** 1837
[3] Kieffer H H and Stone T C 2005 *Astron. J.* **129** 2887
[4] Wagner S C, Hewison T, Stone T, Lacherade S, Fougnie B and Xiong X 2015 *Proc. SPIE* **9639** 96390Z
[5] Grantham S E *et al* 2022 The irradiance instrument subsystem (IRIS) on the airborne-lunar spectral irradiance (air-LUSI) instrument *Meas. Sci. Technol.* **33** 065021
[6] Cataford A, Gadsden S A and Turpie K 2020 *Adv. Space Res.* **65** 2315
[7] Zarobila C J, Grantham S, Brown S W, Woodward J T, Maxwell S E, Defibaugh D R, Larason T C and Turpie K R 2020 *Rev. Sci. Instrum.* **91** 094505
[8] Newton A, Cataford A, Maxwell S E, Gadsden S A and Turpie K 2020 *Acta Astronaut.* **176** 558
[9] Yoon H and Gibson C 2011 *SP250 Spectral Irradiance Calibrations* (Gaithersburg, MD: Special Publication (NIST SP), National Institute of Standards and Technology)
[10] Zong Y, Brown S W, Johnson B C, Lykke K R and Ohno Y 2006 *Appl. Opt.* **45** 1111
[11] White D R, Clarkson M T, Saunders P and Yoon H W 2008 *Metrologia* **45** 199
[12] Shaw P-S, Woodward J T, Johnson B C, Brown S W and Yoon H W 2021 *Appl. Opt.* **60** 10935
[13] Ball C P, Levick A P, Woolliams E R, Green P D, Dury M R, Winkler R, Deadman A J, Fox N P and King M D 2013 *Appl. Opt.* **52** 4806
[14] Woodward J T, Shaw P-S, Yoon H W, Zong Y, Brown S W and Lykke K R 2018 *Rev. Sci. Instrum.* **89** 091301
[15] Coddington O M *et al* 2021 *Geophys. Res. Lett.* **48** e2020GL091709